Performance of some Limiters on the Higher Order Computation of Inviscid Hypersonic Flows

Abhijit Gogoi[1], Paragmoni Kalita[2]

[1]Department of Mechanical Engineering, Indian Institute of Technology Guwahati,
Assam, India-781039.
gogoiabhijit10@gmail.com
[2]Department of Mechanical Engineering, Tezpur University,
Assam, India-784028.
paragmk@tezu.ernet.in

Abstract:*The Advection Upstream Splitting Method (AUSM) is used to compute 2D inviscid hypersonic flow over a semi-cylinder on a finite volume framework. Solution reconstruction to achieve higher order accuracy is done using the MUSCL-type reconstruction technique with the Van Albada and Hemker-Koren limiter functions. The gas models under consideration are the perfect gas model and the high temperature equilibrium chemically reacting air model of Tannehill and Mugge. The performance of these limiters in computing hypersonic flows is analyzed and compared with the first order accurate method.*

Keywords: Hypersonic, shock, reconstruction, limiter**.**

1. Introduction

In this present work, computations of inviscid hypersonic flow of air over blunt bodies are carried out using the finite volume framework. In the context of hypersonic flow, inviscid analysis is found quite relevant for the calculation of pressure coefficients and wave drag coefficients for hypersonic blunt bodies. The Mach number independence principle is also established by the inviscid model [1]. On the other hand, for the analysis of numerical stability of various flux schemes, especially at very high Mach numbers, the numerical solution of the governing equations for inviscid hypersonic flow seems to find great importance over the decades [2, 3, 4, 5, 6, 7,8,9]. This asserts the importance of the inviscid model in the study of hypersonic flows.

In general at hypersonic speeds, the air temperature near the nose portion of the blunt bodies may be high enough to induce chemical reactions like dissociation of oxygen and nitrogen molecules, formation of nitrogen oxide etc. [1]. In that context, we consider the flow to be in vibrational and chemical equilibrium if the vibrational excitation and chemical reactions take place quite rapidly in comparison to the time taken by a fluid element to move through the flow field. In the present work, air is treated both as a perfect gas and a chemically reacting equilibrium gas. For air as a chemically reacting equilibrium gas, polynomial correlations of Tannehill and Mugge [10] are used for calculating the properties of high temperature air. These data are quite widely used for practical computation of properties of high temperature air. The perfect gas model computes the drag coefficient within 2% of that obtained by the equilibrium airmodel. Although perfect gasmodel and equilibrium air model show significant variation with respect to temperature fields, the pressure field obtainedby perfect gas model is found to be within 2% accuracy to that, obtained by equilibrium air model [11].

For the numerical solution of the Euler equations using the finite volume method, either a central or an upwind scheme can be implemented for the computation of the flux term across a cell interface. vanLeer's Flux Vector Splitting [12],

Liou and Steffen's AUSM [2], Steger and Warming's Flux Vector Splitting [13] , Roe's Flux Difference Splitting [14] etc. are some of the popular upwind methods. MacCormack's scheme [15], Local Lax-Friedrichs (LLF) or Rusanov's scheme [16], Jameson et al.'s JST scheme [17] etc. are examples of central schemes. In the present work, the fluxes are computed using the AUSM scheme.

The Godunov's theorem [21] states that monotone linear numerical schemes for solving partial differential equations (PDE's) can be at most first-order accurate. Thus, higher order accurate numericalschemes require non-linear limiter functions, to suppress the numerical oscillations in the regions of high gradients like shocks, i.e. to produce monotone solutions. The limiters reduce the slope used for the interpolation of a variable to the cell face in the regions of strong gradients. So the scheme appears to be first order accurate in the regions of strong gradients, but still maintains higher order accuracy elsewhere. van Leer [18] proposed the MUSCL approach for obtaining higher order accuracy in the finite volume discretization of the flux terms. In the implementation of MUSCL approach, various limiter functions can be used.However, a relative comparison on the performance of different limiter functions in a single source has not been made yet. In this paper, the performance of two limiter functions, namely the Van Albada limiter and Hemker-Koren limiter functions [19] in computing hypersonic flow involving strong shock is investigated. Corresponding improvements are compared with the first order accurate solutions.

This paper is organized in five sections. Section **2** presents the Euler equations of gas dynamics. Liou and Steffen's AUSM scheme and the Equilibrium air model by Tannehill and Mugge are briefly discussed in section **3**. This section also presents the MUSCL technique along with the various limiter functions used in this work. The results and discussion on the various computations are presented in section **4**. The density- and Mach number-contour plots for inviscid hypersonic flow over a semi-cylinder obtained by higher order accurate AUSM scheme using different limiter

functions are presented. Section **5** summarizes the results of the computations done in the present work.

2. The Governing Equations

Set For inviscid flow the governing equations are Euler equations expressed in compact notation as follows [2]:

$$\frac{\partial \mathbf{U}}{\partial t} + \frac{\partial \mathbf{F}}{\partial x} + \frac{\partial \mathbf{G}}{\partial y} = 0 \qquad (1)$$

where, $\mathbf{U} = \begin{bmatrix} \rho \\ \rho u \\ \rho v \\ \rho e_m \end{bmatrix}$ $\mathbf{F} = \begin{bmatrix} \rho u \\ p + \rho u^2 \\ \rho u v \\ (p + \rho e_m) u \end{bmatrix}$ $\mathbf{G} = \begin{bmatrix} \rho v \\ \rho v u \\ p + \rho v^2 \\ (p + \rho e_m) v \end{bmatrix}$

Here **U** is the vector of conserved variables, **F** and **G** are the flux vectors and e_m is the total energy of the fluid per unit mass, rest of the symbols have their usual meanings. Steady state solutions are obtained by solving the above equations through time-marching using the first order Euler explicit method.

3. The Numerical Schemes and the Equilibrium Air Model

3.1 The AUSM scheme

The AUSM scheme considers that the flux vector consists of the convective and accoustic parts. The convective part is associated with the fluid velocity and the accoustic part is due to the pressure component. Accordingly, upwinding of the convective part is done based upon the sign of the contravariant Mach number. The acoustic part depends on both the upstream and downstream pressures for subsonic flow, whereas it becomes fully upwind for supersonic flows only.

$$\mathbf{F} = \mathbf{F}^{(c)} + \mathbf{F}^{(p)}$$

where, $\mathbf{F}^{(c)} = u \begin{pmatrix} \rho \\ \rho u \\ \rho u \\ \rho h_0 \end{pmatrix}$, $\mathbf{F}^{(p)} = \begin{pmatrix} 0 \\ p \\ p \\ 0 \end{pmatrix}$ (2)

Based upon the Mach number obtained at the cell interface, the convective part at the cell interface is computed as,

$$\mathbf{F}_{1/2}^{(c)} = M_{1/2} \begin{pmatrix} \rho a \\ \rho u a \\ \rho v a \\ \rho h_0 a \end{pmatrix}_{L/R} \qquad (3)$$

where $(\bullet)_{L/R} = \begin{cases} (\bullet)_L, \text{if } M_{1/2} > 0 \\ (\bullet)_R, \text{if } M_{1/2} < 0 \end{cases}$

Here the subscript '1/2' refers to the interface between the upstream and downstream sides 'L' and 'R' respectively. The Mach number at the interface is calculated as follows.

$$M_{1/2} = M_L^+ + M_R^-$$

where, $M^{\pm} = \begin{cases} \dfrac{1}{2}\left(M \pm |M|\right), \text{if } |M| \geq 1 \\ \pm \dfrac{1}{4}\left(M \pm 1\right)^2, \text{ otherwise} \end{cases}$ (4)

The pressure at the interface is calculated by using the following expressions

$$p_{1/2} = p_L^+ + p_R^-$$

where, $p^{\pm} = \begin{cases} p\left(\dfrac{M \pm |M|}{2M}\right), \text{if } |M| \geq 1 \\ \dfrac{p}{4}\left(M \pm 1\right)^2\left(2 \mp M\right), \text{otherwise} \end{cases}$ (5)

3.2 The MUSCL apporach and the limiter functions

van Leer's MUSCL (Monotone Upstream-Centred Schemes for Conservation Laws) [18] is one of the methods to reconstruct the left and right states of a cell-face based upon the information in the neighbouring cells. With reference to Fig. 1, the left and right states for the cell-interface '1/2' are given by the following general expression using the MUSCL approach.

$$U_R = U_{I+1} - \frac{1}{2}\psi_R\left(U_{I+2} - U_{I+1}\right)$$

$$U_L = U_I + \frac{1}{2}\psi_L\left(U_{I+1} - U_I\right)$$

(6)

where, $\psi_{L/R} = \frac{1}{2}\left[\left(1+\hat{\kappa}\right)r_{L/R} + \left(1-\hat{\kappa}\right)\right]\Phi_{L/R}$

such that, $r_R = \dfrac{U_{I+1} - U_I}{U_{I+2} - U_{I+1}}$ and $r_L = \dfrac{U_{I+1} - U_I}{U_I - U_{I-1}}$

and $\Phi(r)$ is a slope limiter with the symmetric property,
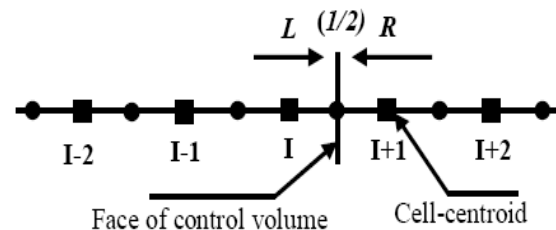
$$\Phi(r) = \Phi(1/r)$$

Figure 1: The left and right states for a cell-face in a cell-centred finite volume method.

The stencil size and the nature of the reconstruction depend on the value of the parameter $\hat{\kappa}$ as shown in Table 1 **[19].**

I. **TABLE 1:** DEPENDENCE OF TYPE OF RECONSTRUCTION ON THE VALUE OF $\hat{\kappa}$

$\hat{\kappa}$	Type of reconstruction
1	Centred
1/3	Upwind-biased
0	Upwind-biased
-1	Upwind

In case of the Van Albada limiter, $\hat{\kappa} = 0$ and the slope limiter function is taken as,

$$\Phi(r) = \frac{2r}{r^2+1} \quad (7)$$

In this case the function $\psi(r)$ corresponds to the Van Albada limiter where,

$$\psi(r) = \frac{r^2+1}{1+r^2} \quad (8)$$

With this definition for $\psi(r)$, the left and right states of the cell-interface is calculated using the Van Albada limiter as ,

$$U_R = U_{I+1} - \frac{1}{2}\delta_R$$

$$U_L = U_I + \frac{1}{2}\delta_L \quad \textbf{(9)}$$

Conventionally, the function δ is the same for both the states given by,

$$\delta = \frac{a(b^2+\varepsilon) + b(a^2+\varepsilon)}{a^2+b^2+2\varepsilon} \quad (10)$$

so that,

$$a_R = U_{I+2} - U_{I+1}, \ b_R = U_{I+1} - U_I \quad (11)$$

$$a_L = U_{I+1} - U_I, \ b_L = U_I - U_{I-1}$$

The additional parameter ε is required to prevent the activation of the limiter in smooth flow regions due to small-scale oscillations. It has to be set proportional to the local grid scale. In the present work it is taken as,

$$\varepsilon = 10 \times (\Omega)^{1.25}, \text{ where } \Omega \text{ is the cell volume (12)}$$

In case of the Hemker and Koren limiter function, $\hat{\kappa} = 1/3$. The slope limiter is given by,

$$\Phi(r) = \frac{3r}{2r^2 - r + 2} \quad (13)$$

Following the way as in case of the previous limiter, the reconstruction formula using the Hemker and Koren limiter becomes of same form as equation (9), with the function δ now having the form,

$$\delta = \frac{(2a^2+\varepsilon)b + (b^2+2\varepsilon)a}{2a^2 + 2b^2 - ab + 3\varepsilon} \quad (14)$$

The definitions of the parameters a, b and ε are retained as in equations (11) and (12).

3.3 The equilibrium air model of Tannehill and Mugge

For a given free stream Mach number, computations are initiated by a prescribed value of γ. As the iterations proceed, γ is calculated using density and internal energy per unit mass, which are given by Euler solver. Remaining thermodynamic properties such as pressure, sonic velocity and temperature are calculated using correlated formulae suggested by Tannehill and Mugge.

4. Results and Discussion

Flow of air over a semi-cylinder at Mach number 15.0 [20] is considered. The cylinder diameter is 10 m. A strong bow shock is formed ahead of the semi-cylinder at a stand-off distance δ.
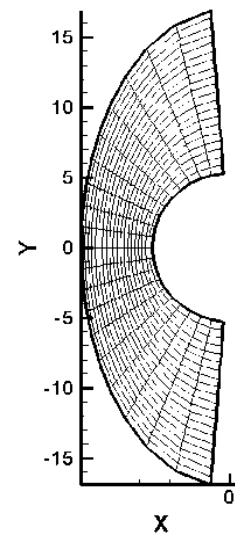

Figure 2: A typical coarse grid for the computation of hypersonic flow over a semi-cylinder.

For flows over such blunt bodies where the shock layer is thick, the inviscid flow assumption also produces reasonably accurate results. A structured grid is used for the computations. A typical coarse grid is shown in Fig. 2. For the actual computations a 201x201 grid along the *r-θ* is taken.

Figure 3 shows the density contour plots at the steady state computed using the first order AUSM, second order AUSM with the Van Albada limiter and second order AUSM with the Hemker-Koren limiter for the perfect gad model as well as for the equilibrium air model of Tannehill and Mugge. From Fig. 3, one important observation is that the shock stand-off distance is less for the equilibrium air model as compared with the perfect gas model. As expected, the shock is found to be slightly better resolved using the second order methods as compared with the first order method. The contour plots don't reveal any remarkable difference between the corresponding results of the Van Albada and Hemker-Koren limiter functions.
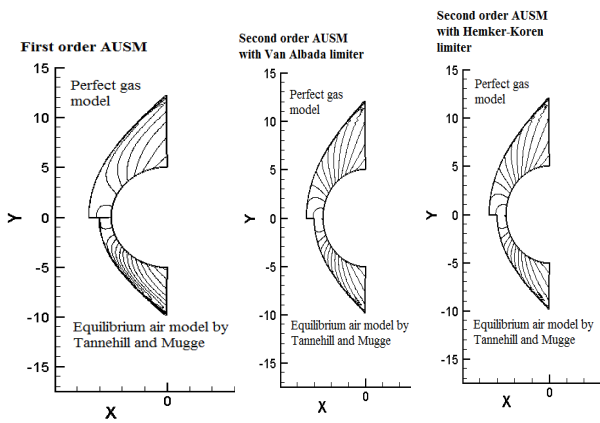
Figure 3: Steady state density contour plots.

The pressure contour plots for the two gas models are shown in Fig. 4. The contour plots for other variables like temperature, Mach number etc. also show similar trend and are not shown in this paper.
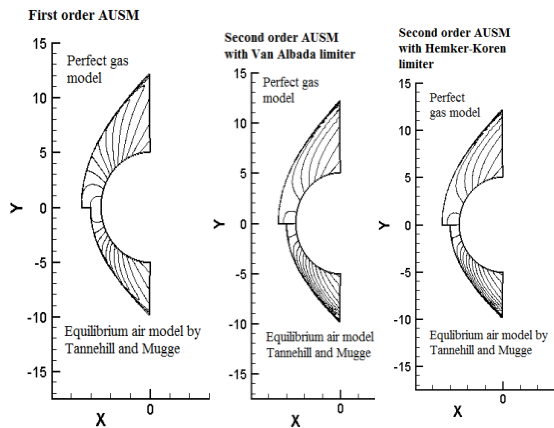

Figure 4: Steady state pressure contour plots.

The variation of normalized density along the stagnation line for the perfect gas model is shown in Fig. 5(a). Due to very strong shock generated at the high Mach number of 15,numerical oscillations are generated at the foot of the shock. The first order scheme does not use any limiter function.It is known that the limiter functions are used to suppress thenon-monotonicity of the numerical solutions.Here it seen that these oscillations are more for the first order scheme as compared with the second order counterparts using thelimiter functions.Overall, both the Van Albada and Hemker-Koren limiter functions are found to produce similar results.However, on a more resolved scale the numerical oscillations are found less for the Van Albada limiter than for the Hemker-Koren limiter.

Figure 5(b) shows the variation of the variation of the non-dimensionalized density along the stagnation line for the equilibrium air model of Tannehill and Mugge for the three methods. It is evident that the shock stand-off distance ismuch less for the equilibrium air model than the perfect gas model. Here also, the numerical oscillations at the foot of the shock are found more with the first order method than the second order methods along-with limiter functions.

The Mach number variation along the stagnation line for the perfect gas model and the equilibrium air model are shown in

Fig. 6(a) and 6(b) respectively. The reduction in shock stand-off distance in case of the equilibrium air model is depicted in these figures also.
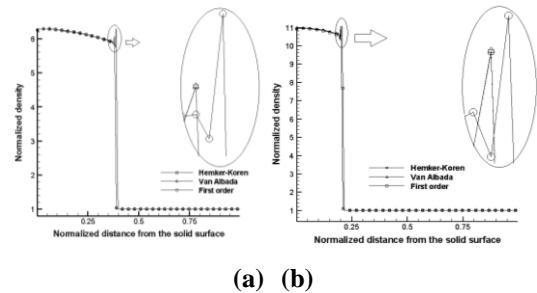

(a) (b)

Figure 5: Variation of density along the stagnation line (a) Perfect gas model (b) Equilibrium airModelof Tannehill and Mugge.

5. Concluding Remarks

Hypersonic inviscid flow over a semi-cylinder is computed for a freestream Mach number of 15.0 using the first order AUSM scheme and the second order AUSM scheme with Van Albada limiter and Hemker-Koren limiter. Results using both the perfect gas model as well as the equilibrium air model by Tannehill and Mugge are presented, compared and analyzed. The computed shock stand-off distance is found less for the equilibrium air model as compared with the perfect gas model. The first order scheme is found toproduce more numerical oscillations, especially for the density computations in the vicinity of the strong shock as compared with the second order schemes with the limiter functions. The performances of the two limiters are found identical for this case. However, on a much resolved scale, the Van Albada limiter is found to suppress the numerical oscillations more than the Hemker-Koren limiter. Some higher order reconstruction techniques with other limiter functions may be tried for such strong shock problems and a more detailed error analysis for all these schemes may be carried out in future.

References

[1] J. D. Anderson Jr., Hypersonic and High Temperature Gas Dynamics, McGraw Hill, pp. 13-24, 1989.

[2] M. S. Liou and C. J. Steffen, Jr., "A new flux splitting scheme," J. Comput. Phy., vol. 107, pp. 23-39, 1993

[3] S. Jaisankar and S.V. Raghurama Rao, "Diffusion regulation for Euler solvers," J. Comput. Phy., vol. 221, pp. 577–599, 2007.

[4] M. Pandolfi and D. Ambrosio, "Numerical instabilities in upwind methods: Analysis and cures for the 'Carbuncle' phenomenon," J. Comput. Phy., vol.166, pp. 271-301, 2001.

[5] M. S. Liou, "Mass flux schemes and connections to shock instability," J. Comput. Phy., vol. 160, pp. 623-648, 2000.

[6] M. Dumbser, J. Moschetta and J. Gressier, "A matrix stability analysis of the carbuncle phenomenon," J. Comput. Phy., vol. 197, pp. 647-670, 2004.

[7] J. Li, Q. Li and K. Xu, "Comparison of the generalized Riemann solver and the gas-kinetic scheme for inviscid compressible flow simulations," J. Comput. Phy., vol. 230, pp. 5080-5099, 2011.

[8] K. Kitamura,and E. Shima, "Towards shock-stable and accurate hypersonic heating computations: A new pressure flux for AUSM-family schemes," J. Comput. Phy., vol. 245, pp. 62-83, 2013.

[9] P. Kalita and A.K. Dass, "Computations of high speed flows using diffusion regulation," Fortieth National Conference on Fluid Mechanics and Fluid Power, NIT Hamirpur, Paper ID 185, 2013.

[10] J. C. Tannehill and P. H. Mugge, "Improved curve fits for the thermodynamic properties of equilibrium air suitable for numerical computations using time-dependent or shock-capturing methods," NASA, CR-2470, 1974.

[11] S. M. Deshpande, "Boltzmann schemes for continuum gas dynamics," Sadhana, vol. 18, pp. 405-430, 1993.

[12] W.K. Anderson, J.L. Thomas and B. van Leer, "Comparison of finite volume flux vector splitting for the Euler equations," AIAA J., vol. 24, No. 9, pp. 1435-1460, 1986.

[13] J. L. Steger and R.F. Warming, "Flux vector splitting of the inviscid gas dynamic equations with9the application to finite difference methods," J. Comput. Phy., vol. 40, pp. 263-293, 1981.

[14] P. L. Roe, "Approximate Riemann solvers, parameter vectors and difference schemes," J. Comput. Phy., vol. 43, pp. 357-372, 1981.

[15] R. W. MacCormack, "The effect of viscosity in hypervelocity impact cratering," AIAA Paper, Cincinnati, Ohio, pp. 69-354, 1969.

[16] R. J. LeVeque, Finite volume methods for hyperbolic problems, Cambridge texts in Applied Mathematics, first edition, Cambridge University Press, pp. 232-234, 2002.

[17] A. Jameson, "Analysis and design of numerical schemes for gas dynamics 1: Artificial diffusion, upwind biasing, limiters and their effect on accuracy and multigrid convergence," Int. J. Comput. Fl. Dyn., vol. 4, pp. 171–218, 1995.

[18] B. van Leer, "Towards the Ultimate Conservative Difference Scheme V. A Second Order Sequel to Godunov Method," J. Comput. Phy., vol. 32, pp. 101-136, 1979.

[19] J. Blazek, Computational fluid dynamics: Principles and applications, Elsevier, pp. 267-293, 2001.

[20] R. Kumar and A. K. Dass, "Aspects of computation of hypersonic flow over blunt bodies," Proceedings of the 4th International and 37th National Conference on Fluid Mechanics and Fluid Power, IIT Madras, Paper ID FMFP10-HS-04, 2010.

[21] S. K. Godunov, "A Difference Scheme for Numerical Solution of Discontinuous Solution of Hydrodynamic Equations," Math. Sbornik, vol 47, pp. 271-306, 1959.

Authors Profile

Abhijit Gogoi, is a research scholar in the Department of Mechanical Engineering, Indian Institute of Technology, Guwahati , India. He received his master degree in Applied Mechanics from Tezpur University (India) in 2015.

ParagmoniKalita,is working as an Assistant Professor in the Department of Mechanical Engineering, Tezpur University, India. He received his master degree in Heat Power Engineering form Banaras Hindu University, Varanasi (India) in 2004. He is pursuing his Phd degree from Indian Institute of Technology, Guwahati, India.